# Maximizing two-dimensional liquid chromatography peak capacity for the separation of complex industrial samples

Zhu, Koudi; Pursch, Matthias; Eeltink, Sebastiaan; Desmet, Gert

*Published in:*
Journal of Chromatography A

*DOI:*
10.1016/j.chroma.2019.460457

*Publication date:*
2020

# Maximizing 2D-LC Peak Capacity for the Separation of Complex Industrial Samples

Koudi Zhu [a,c], Matthias Pursch [b], Sebastiaan EELTINK [c], Gert Desmet [c,*]

[a] DuPont Nutrition & Health, Larkin 200, Midland, MI 48674
[b] Dow Stade Produkt. GmbH&Co OHG, Analytical Sciences, 21677 Stade, Germany
[c] Department of Chemical Engineering, Vrije Universiteit Brussel, Pleinlaan 2, 1050 Brussel, Belgium

∗Corresponding author e-mail addresses: gedesmet@vub.be

**Abstract**

We report on a study on the use of 2D-LC in industry wherein we maximized the peak capacity by serially coupling up to six 15cm long columns in the 1st dimension. For the considered aromatic amine oligomer sample, the combination of reverse phase pentafluorophenyl (Phenomenex Kinetex F5) columns in the 1st and a more retaining reverse phase polymeric C18 (Agilent PAH) column in the 2nd dimension proved to give the highest orthogonality, calculated to be 0.82. Whereas a 1D run on a single column revealed around 120 compounds, the optimized 2D LC system revealed around 940 compounds. To achieve this, flow splitting to improve the peak capacity in the 1st dimension and shifting gradients in the 2nd dimension were used. The overall peak capacity of the system was calculated to be 53000 and 11000, respectively, without and with correction for orthogonality and undersampling. Total analysis time with the 6-column system was around 20 hrs.

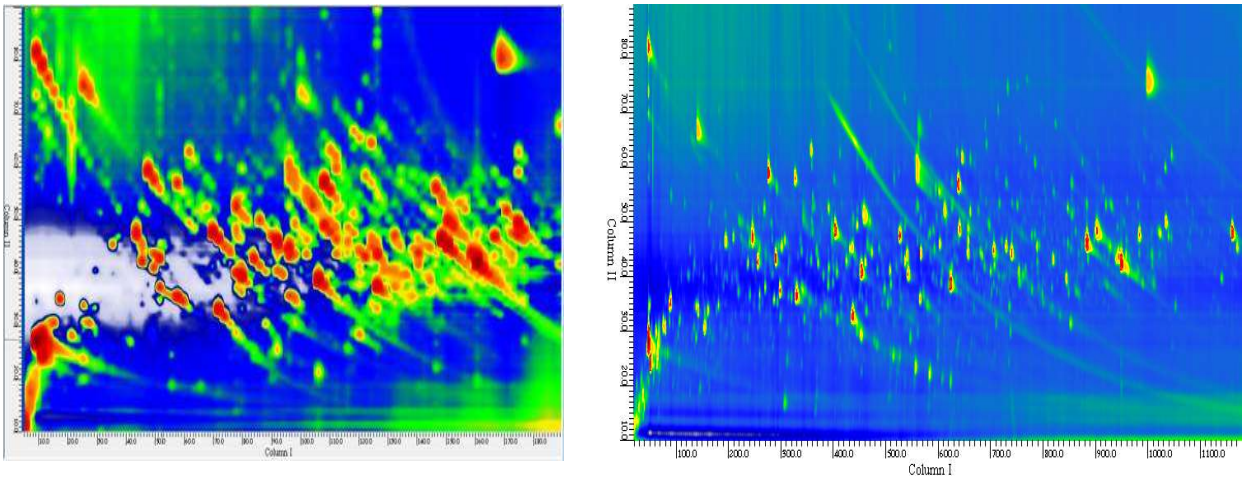


One F5 column in 1D ⟹ Six F5 columns in 1D

## 1. Introduction

The essence of a chromatography separation is to resolve peaks. The resolving power of a liquid chromatography system can be conveniently expressed by peak capacity, i.e., maximum number of peaks resolvable from each other in the separation time or space domain [1]. The peak capacity is roughly proportional to the root square of the column efficiency. In gradient LC, peak capacity $n_c$ is related to the column efficiency and operating parameters as derived by Snyder (Eqs 1 and 2) where N is the column efficiency, $\Delta\varphi$ is the mobile phase organic modifier percentage change, S is slope of the linear regression of logk vs $\varphi$ which is analyte dependent ($\log k = \log k_W - S\varphi$), k is the retention factor, $k_W$ is an extrapolated retention factor where water is used as the mobile phase, b is a parameter defined by column void time $t_0$ and gradient time $t_G$ (Eq 2) [2].

$$n_c = (2.3/4)\, N^{\frac{1}{2}} \Delta\varphi^2\, S/(2.3b + 1) \quad (1)$$

$$b = t_0 \Delta\varphi / t_G \quad (2)$$

If we assume a shallow gradient running from 10 to 90% organic modifier ($\Delta\varphi$ = 0.9 - 0.1=0.8 with $t_G/t_o$ = 20) for the separation of small molecules (S= 4), the peak capacity in Equation 1 is approximated to be 1.3 times the root square of the column efficiency. For a difficult separation, a high column efficiency such as 100,000 plates might be needed, which could generate a peak capacity of roughly 400 for small molecules. A large peak capacity of ~1000 could be theoretically obtained for oligomers which have large S value due to their large molecular weight.

It seems straightforward to increase peak capacity by increasing column efficiency. However, in addition to the resolving power, separation time is of importance as well, especially in an industrial setting. The fundamental relationship regarding the separation speed and efficiency was elegantly treated by Knox and Saleem, and Poppe (Eq 3), where E is the separation impedance, ($E = h^2 Ø$, ~3000-4000 under optimized condition; h is reduced plate height and Ø is the column resistance factor which is a constant, 500~1000 for a packed column), $\eta$ is mobile phase viscosity, and $\Delta$P is the column pressure drop [3,4]. As can be seen, an increase in efficiency is at constant $\Delta$P inevitably accompanied by a large increase in separation time when operated at optimum conditions.

$$t_o = EN^2\eta/\Delta P \quad (3)$$

$$d_p(opt) = \sqrt{\frac{\phi\eta D \nu_{min} h_{min} N_r}{\Delta P}} \quad (4)$$

Eq 4 shows the optimum particle diameter for a required column efficiency $N_r$ where $\eta$ is the mobile phase viscosity, D is the analyte diffusion coefficient, $\nu_{min}$ is the optimal reduced velocity, $h_{min}$ is the minimum reduced plate height. It is interesting that to achieve a large plate number with fixed pressure, a large particle diameter must be used in order to have the shortest separation time.

In the early days of chromatography, due to the instrumentation pressure limit of 400 bar, 5 µm or 7-8 µm particle with very long column were used to generate up to 1 million plates [5-7]. However, the column void time approached a few hours to 18 hours, making this approach unpractical for achieving a

large peak capacity. Modern instrumentation has the capability of providing up to 1500 bar pressure, making it possible to attain 100,000 plates, resulting in peak capacity of ~1000 in relatively short time with a column void time of a few minutes by using long core-shell 2.7 um particle or total porous sub-2 um particle [8-11]. However, the nominal peak capacity does not equate to the number of analytes that can be resolved. Based on the peak overlap theory, a peak capacity of 1000 is required to have a sufficient chance (90% probability) to observe only 50 peaks in a chromatogram as a singlet (i.e., not co-eluted with other analytes) [12]. For highly complex samples, such as those in the fields of proteomics, pharmaceutical, chemical industry the situation is even more dramatic. For example, for a sample containing 1000 compounds, a very large peak capacity in the order of 20,000 might be required for completely resolving them. To achieve such a high peak capacity, column efficiencies in the range of N=40 million would be required, as inferred from Eq 1. This is obviously in-practical as the run time would be prohibitively long. Thus, other strategies must be sought to achieve an order of magnitude improvement in the peak capacity (ie, from 1000 to 10,000).

Giddings, in his theoretic treatment, conceptualized the power of two-dimensional LC (2-D LC) where the overall peak capacity of 2-D LC is the product of the peak capacity in each dimension if the separation in the two dimensions are orthogonal [13]. An early demonstration of comprehensive 2D-LC was conducted for the separation of a 14-component mixture of proteins using a combination of size exclusion chromatography and ion exchange chromatography [14]. Recently, 2-D LC has become more and more attractive due to its ability to separate complex samples, such as proteomic [15-24], metabolomics [25, 26], surfactant/ polymer/nanoparticles [27-30], and pharmaceutical molecules [31-33]. The wide use of 2-D LC is facilitated by the commercialization of 2-D LC instrumentation which makes data acquisition and analysis user-friendly. Although one main area focuses on developing 2-D LC method with short total run time [19,21,32,34-37], there is also a strong need to develop more generic 2D-LC methods with a large peak capacity, especially for the industrial samples that might only be analyzed once for process troubleshooting or process improvement. Hence, a maximum peak capacity is desirable while the total time can be slightly sacrificed as long as it is not excessively long.

In an ideal situation, 2D-LC peak capacity can be calculated following the product rule: $n_{c,2D} = {}^1n_c \times {}^2n_c$ [13]. The effective peak capacity $n_{c,2D}^{eff}$ , however, must be corrected by incomplete surface coverage $f_{coverage}$ and under-sampling correction factor $\langle\beta\rangle$ as shown in Eqs 5 and 6 where ${}^2t_s$ is the ${}^2$D cycle time, or called ${}^2$D modulation time, ${}^1\sigma$ is the first dimension peak standard deviation equating to ¼ of the peak width ${}^1$w [38].

$$n_{c,2D}^{eff} = {}^1n_c \, {}^2n_c f_{coverage} \frac{1}{\langle\beta\rangle} \quad (5)$$

$$\langle\beta\rangle = \sqrt{1 + 0.21( {}^2t_s / {}^1\sigma)^2} \quad (6)$$

The ${}^1n_c$ and ${}^2n_c$ can be measured from the experimental data by using $1+t_G/w$, or any of the many possible more accurate metrics [39]. Several approaches have been proposed to calculate the 2D surface coverage, including bin-counting, ecological home-range theory, fractal mathematics and Asterisk Equation metric [40-44]. In this paper we chose to use the Asterisk Equation metric method, as it is less sample dependent and well considers the peak spreading in both dimensions [44]. This method

is also easy to be implemented by exporting data from the LC image software to a Microsoft Excel spreadsheet for calculation.

Several optimization strategies for comprehensive 2-D LC have been reported and summarized in a recent review article [45]. Gu et al reported two-step or one-step optimization [46]. In two-step optimization, the peak capacity in $^{1}$D was maximized and then overall peak capacity was optimized. In one-step optimization, all the parameters are changed simultaneously to achieve the maximum overall peak capacity. A more elegant way based on Pareto-optimality approach was also reported where a systematic approach based on pilot run and then model build to optimize peak capacity, total run time and dilution factor at the same time [47]. The Pareto-optimality approach has the advantage of a "dry-run" simulation but a model must be established first and a home-built MATLAB routines must be used.

When accounting for the f- and $\beta$-factor, the effective peak capacity can be significantly lower than the multiplication of the peak capacity from $^{1}$D and $^{2}$D. To explore the potential of a comprehensive 2D-LC to see whether it can attain an order of improvement in peak capacity to 10,000, we report on a study wherein we attempted to maximize the peak capacity by serially coupling up to six 15cm long columns in the 1$^{st}$ dimension. To emphasize the practical relevance of the work, this was done on an industrial aromatic amine oligomer sample. To allow connecting a sufficient number of columns in series within the pressure limits of the instrumentation (1200 bar), 2.6μm core-shell particles were used in the $^{1}$D. The $^{2}$D was a 5cm 1.8μm particle column.

## 2. Experimental

An Agilent 1290 Infinity 2D-LC system (Agilent, Santa Clara, CA) was used for all experiments in this study. The system was comprised of an Infinity 1290 quaternary pump (G4204A), an Infinity 1290 autosampler (G4226A), an Infinity 1290 thermostatted column compartment (G1316C), and 1260 diode-array detector with a high-pressure flow cell (G1315C, 400 bar, 6mm pathlength, 1.7 μL flow cell volume) in $^{1}$D. An Infinity 1290 binary pump (G4220A), an Infinity 1290 thermostatted column compartment (G1316C), an Infinity 1290 diode-array detector (G4212A) equipped with an Agilent Max-Light Cartridge Cell (60 mm pathlength, 1.0 μL flow cell volume) in $^{2}$D. Interface for the 2D LC is a 2-position 10-port active solvent modulation valve (ASM, G1170A) with 40 or 70 μL loop. The ASM function is not activated in this study.

To protect columns, Agilent 1290 Infinity in-line filters were used in front of the columns in both dimensions. For $^{1}$D, up to six Phenomenex F5 (00F-4723-AN, 150 × 2.1 mm, 2.6-μm core-shell particles, 100-Å pore size) columns were coupled. For $^{2}$D, an Agilent Zorbax Eclipse PAH (959757-318, 50 × 3.0 mm, 1.8-μm totally porous particle) column was used. For flow splitting, Advantage™ SS Tee, 0.25mm Thru-hole (1602, Analytical Sales & Services, Inc.) was connected via 0.05'' stainless steel tubings between the $^{1}$D detector and the ASM valve. The other outlet of the Tee was connected to a PEEK tubing to achieve a split ratio of 4 (ie, 4/5 of the $^{1}$D eluent was directed to waste). 10 mM ammonium bicarbonate buffer at pH 8, and Acetonitrile were used in both dimensions as mobile phases A and B, respectively. The system was controlled with an Agilent OpenLAB CDS Chemstation Edition (Rev. C.01.07 SR3 [465]) software. Data were exported to GC Image ™ Version 2.5b0 LC X LC for processing. For MS data collection, 0.05''-id PEEK tubing was used to connect the $^{2}$D detector to an

Agilent 6130 Single-Quad mass spectrometry via a Tee (Advantage™ PEEK™ Tee, 0.01" ID, 1625, Analytical Sales & Services, Inc.) to have a 1:1 split ratio.

Approximately 50 mL of an aromatic amine oligomer sample was obtained in-house from the Dow Chemical Company. The sample was diluted in N, N-dimethylformamide (DMF) (Fisher Chemical) roughly 10 times and then filtered with 0.2 µm PFTE filter (Fisher Brand, 25 mm syringe filter, 09-719 G). 2 µL of the filtered solution was injection for LC run.

## 3. Results and Discussion

Several column pairs including Waters BEH C8/Waters BEH C18, Agilent HPH C18/ Agilent PAH, and Phenomenex F5/Agilent PAH were screened for use as $^{1}$D and $^{2}$D column, respectively. Preliminary data found F5/PAH pair the most promising in regards to peak shape and surface coverage, and they were chosen for further optimization. The Phenomenex F5 column, which is a pentafluorophenyl phase, promotes $\pi$-$\pi$ interaction as the sample consists of aromatic amine oligomers. The Agilent PAH column , a polymeric C18 phase, provides more retention, so that the analytes eluting out of the $^{1}$D will be focused on the $^{2}$D column even when large volumes (i.e., 40, or 70 µL) is injected. In addition, it was anticipated the PAH phase would display a significantly different selectivity than the F5 phase.

Since the aromatic amine (protonated form) has a $pK_a$ of 4.6 at 25 °C, the retention will be minimal in acidic mobile phase with pH less than 3.6. We chose 10 mM ammonium bicarbonate buffer at pH 8 as the mobile phase A to keep the aromatic amine oligomers in non-protonated form and have good retention on the columns in both dimensions. The effect of column temperature was screened, finally making us select 30 °C for $^{1}$D and 50 °C for $^{2}$D.

We used the two-step approach with slight modification for optimization of the 2-D LC and reported it in the following sections [46].

### *3.1 1D separations*

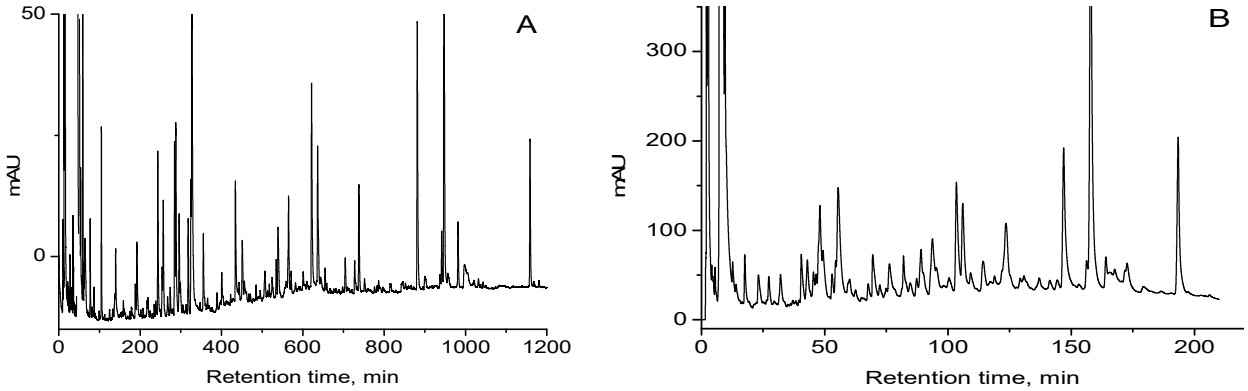


**Figure 1.** 1D chromatogram of aromatic amine oligomer sample. Conditions for panel A: F5, 2.6 µm, 900 x 2.1 mm; Mobile phase A: 10 mmol ammonium bicarbonate, pH 8; Mobile phase B: ACN; Flow rate: 0.15 mL/min; Temperature: 30 °C; Gradient: 15% to 65% B over 1180 min; $t_0$=14.5 min. Conditions for panel B: F5, 2.6 µm, 150 x 2.1 mm; Gradient: 15% to 65% B over 196 min. Other conditions: same as in panel A.

The column flow rate and gradient time $t_G$ were optimized for the six coupled core-shell columns. The optimum linear velocity was calculated to be ~1.15 mm/s using Eq ($u = vD/d_p$) assuming ν=3 and D=$10^{-9}$ $m^2$/s, respectively. Considering the column diameter and assuming column porosity of 0.7, this linearity velocity translates into a volumetric flow of 0.167 mL/min with a corresponding $t_o$ of 13 min. For convenience, a column flow rate of 0.15 mL/min, close to the optimum flow rate, was chosen with a corresponding $t_0$ of 14.5 min. Pressure drop at this condition was about 1100 bar. To maximize peak capacity, a very shallow gradient with $t_G$ of 1180min ($t_G/t_0$ of ~80,) was chosen. Figure 1A shows the separation of the aromatic amine oligomer sample using six F5 columns. Selecting 13 peaks that seem absent from coelutions and then calculate the average peak width, the peak capacity was measured to be 1263. In contrast, the use of one F5 column ($t_0$=2.4) is shown in Figure 1B for the same flow rate and same $t_G/t_o$. The peak capacity was calculated to be 352 only. The ratio of both peak capacities (3.6) is larger than the theoretically expected $\sqrt{6}$. This indicates the peaks selected in the single column case as being supposedly singlet peaks probably still contained overlapping compounds. Fig. 1 clearly demonstrates the advantage of using 6 instead of 1 column. In the 1 column chromatogram, 120 different peak features can be detected, while in the 6-column case this amount increases significantly to 330 detected features.

### *3.2 2D separations*

Figure 2 shows one of the exploratory 2D runs. To shorten the overall run time for speeding up the method development, only two coupled F5 columns were used in the $^1$D. Because no flow splitting was used in the $^1$D and the sample loop volume was 40 µL, the column flow was reduced to 0.02 mL/min, which is obviously too slow but it allows for an adequate cycle time for $^2$D run as the loop fill time is 2 min. This shows one challenge for comprehensive 2-D LC as the $^1$D and $^2$D flow rates are inter-related.

For the $^{2}$D, the column flow rate was 1.5mL/min, which had $t_o$ of 0.164 min. For the $^{2}$D, we selected a gradient time corresponding to $t_G/t_0$ of 10 and a column equilibration time equal to two times $t_o$, resulting in $^{2}$D cycle time of 1.97 min, which is compatible as the $^{1}$D loop filling time was 2 min. The same design principle, i.e. keeping the $^{2}$D cycle time slightly smaller than the $^{1}$D loop filling time so that no sample loss would occur, was used throughout this study. Due to the slow flow rate of only 0.02 mL/min for $^{1}$D, the void time was 36 min even for the two coupled columns. We run ~360 min gradient for the $^{1}$D, resulting in only ~10 for $t_G/t_0$, which is definitely not long enough. A simple gradient of 20-100% B was used in each $^{2}$D. The analytes eluted around the diagonal in the 2D contour plot and the surface coverage of this separation was calculated to be 0.59, using the Asterisk Equation metric method [44].

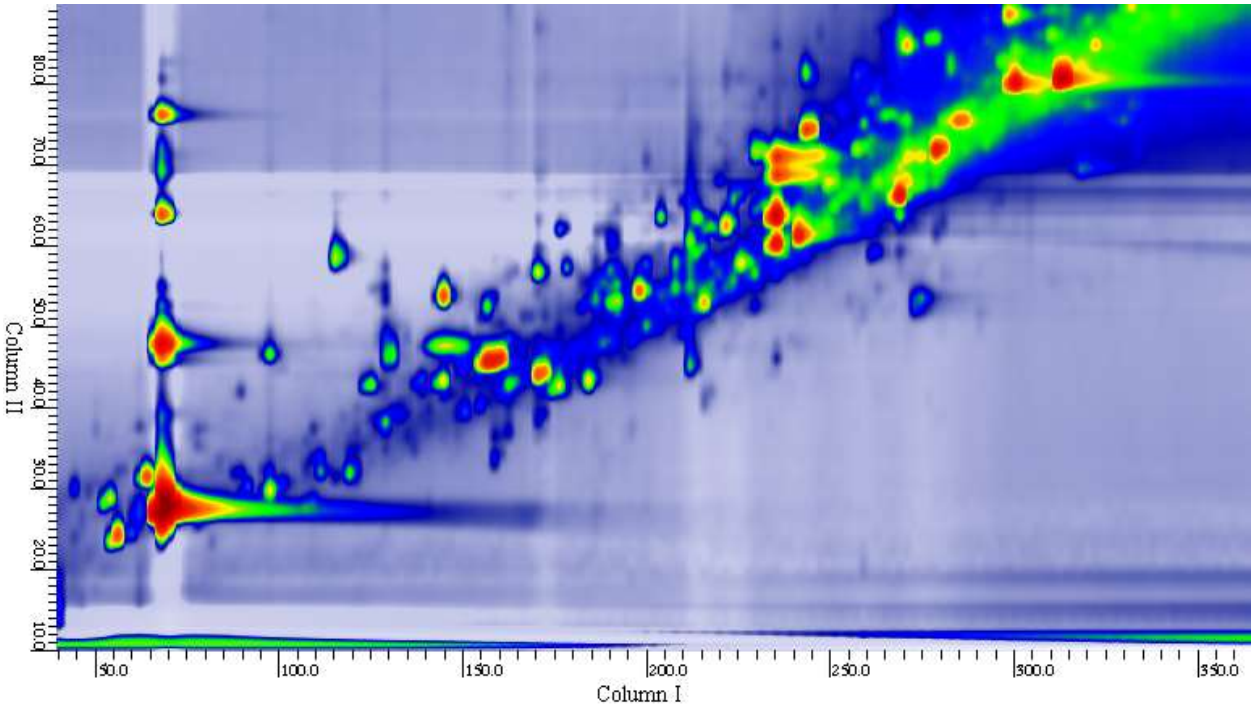


**Figure 2.** 2D-LC contour plot of aromatic amine oligomer sample. Conditions: $^{1}$D, two coupled F5 column, 0.02 mL/min, 20-95% B over 364min, column temperature of 30 °C. $^{2}$D, PAH column, 1.5 mL/min, 20-100% B over 1.65 min, cycle time of 1.97 min, column temperature of 40 °C.

This kind of low surface coverage is characteristic for comprehensive reversed-phase x reversed-phase 2-D LC. One approach to improve the orthogonality is to use a carbon clad phase as the $^{2}$D column [48]. A more convenient way, quite convincingly, is to optimize the gradient in the $^{2}$D [49,50] using the shifted gradient capability of the instrument. As seen from Figure 3, a significant improvement in surface coverage was obtained by applying a shifted gradient for the $^{2}$D run. The concept of a shifted gradient is that the starting and ending mobile phase composition for each $^{2}$D run changes during the whole 2-D LC run (see caption to Fig. 3 for exact conditions). Surface coverage was calculated to be 0.75 under these method conditions. To improve $t_G/t_0$, the column flow rate in $^{1}$D was increased to 0.04 mL/min, which resulted in a shorter loop-filling time. The $^{2}$D column flow rate was proportionally increased to 3

241 mL/min. Column temperature was increased to 50 °C in order to keep the column pressure under 1200
242 bar instrument pressure limit.

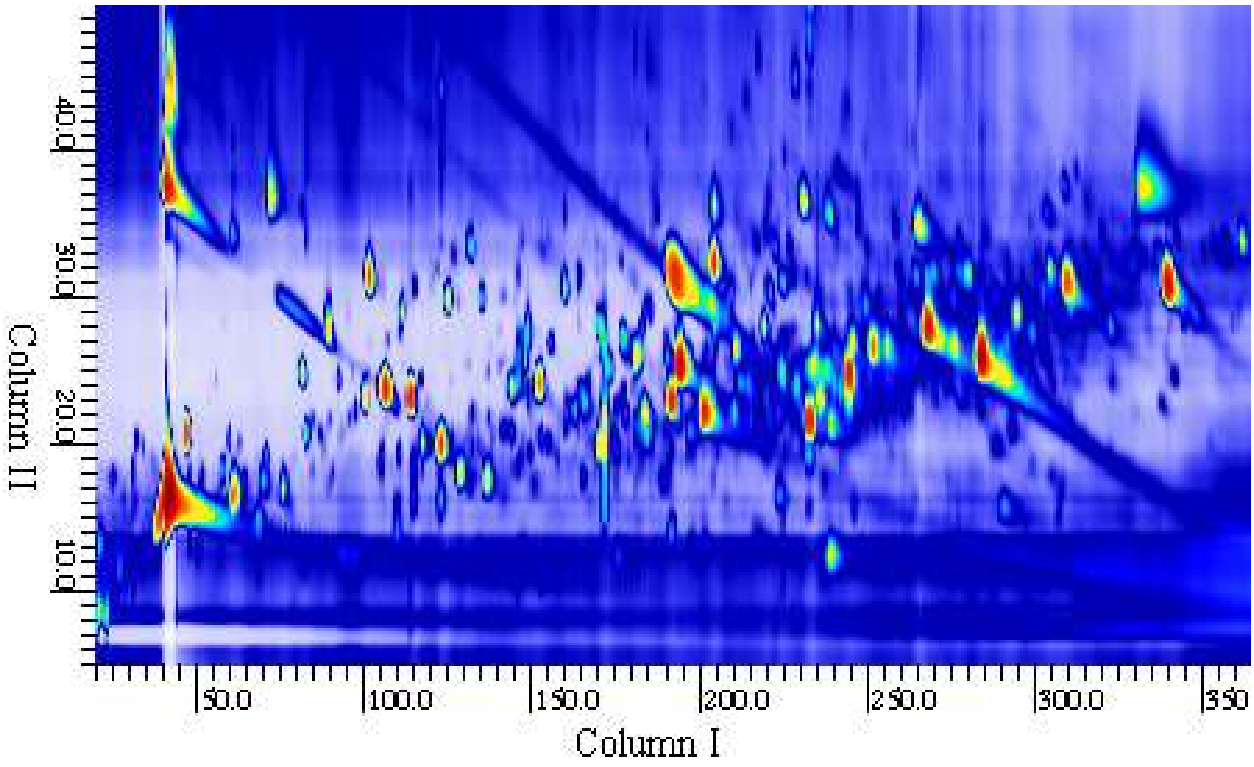


243

244 **Figure 3.** 2D-LC contour plot of aromatic amine oligomer sample using a shifted gradient in $^{2}D$.
245 Conditions: $^{1}D$, two coupled F5 column, 0.04 mL/min, 20-95% B over 364min, column temperature of 30
246 °C, $t_0$ = 18 min. $^{2}D$, PAH column, 3.0 mL/min, 10-40% B in the beginning of 2-D run (shifted to 80-100%
247 over 364 min in the ending of 2D run), the $^{2}D$ gradient time of 0.83 min, cycle time of 0.99 min, column
248 temperature of 50 °C.

249

250

### 3.3 Overall Peak Capacity Optimization

Based on the satisfactory surface coverage obtained as shown in Figure 3, six coupled F5 columns in $^{1}$D and the same PAH column in $^{2}$D were used to attain a higher overall 2-D LC peak capacity. The $t_0$ was increased to 59 min. To maintain similar $t_G/t_0$, the gradient time was increased to 1180 min. As shown in Figure 4, the surface coverage was 0.69, not as good as in Figure 3. The $^{1}$D peak capacity was 528 and $^{2}$D peak capacity was 24.4. The under-sampling factor was 1.17. Using Eq. (5), the overall corrected 2D peak capacity was 7600.

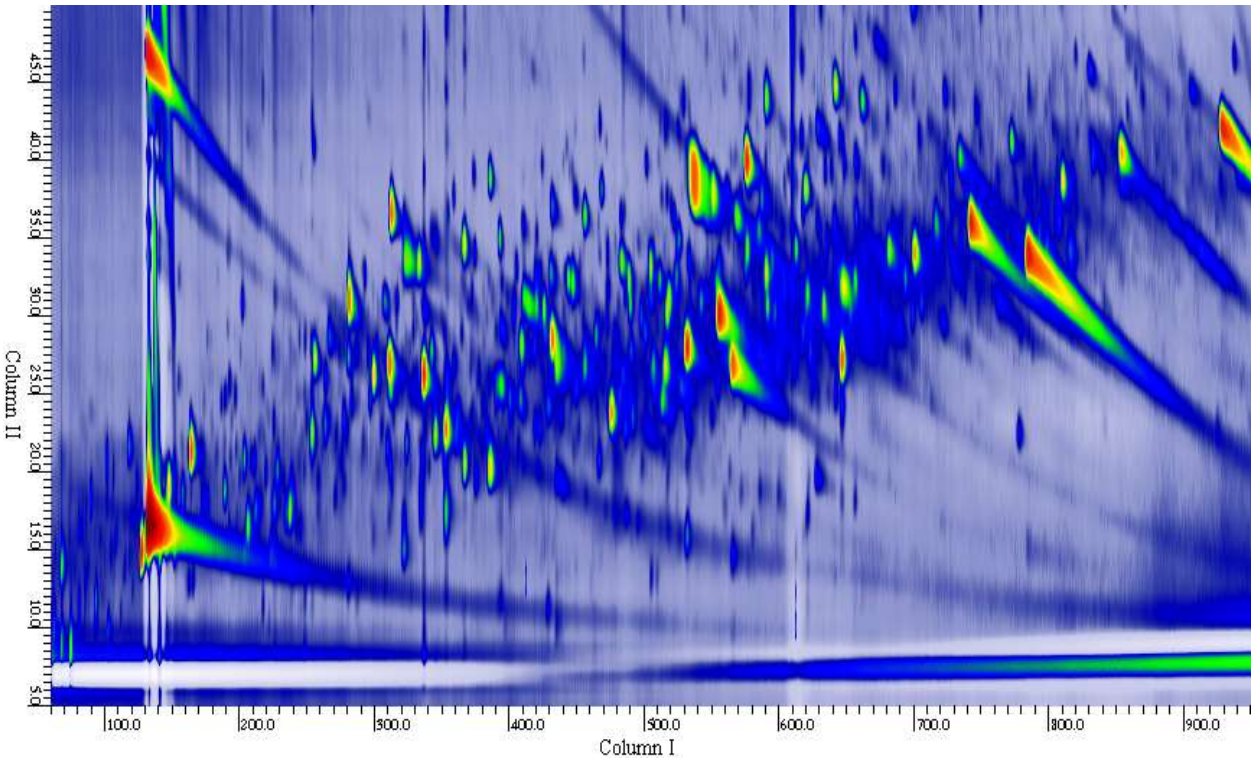


**Figure 4.** 2D-LC contour plot of aromatic amine oligomer sample using six F5 columns in $^{1}$D. Conditions: $^{1}$D, six coupled F5 column, 0.037 mL/min, 20-95% B over 1180 min, column temperature of 30 $^{o}$C. Note that $t_0$ = 59 min. $^{2}$D, PAH column, 3.0 mL/min, 10-25% B in the beginning of 2-D run (shifted to 80-100% over 1180 min in the ending of 2D run), the $^{2}$D gradient time of 0.83 min, cycle time of 1.07 min, column temperature of 50 $^{o}$C.

Encouraged by the peak capacity of 7600 as shown in Figure 4, it was attempted to further increase the 2-D LC peak capacity by improving $^1n_c$, $^2n_c$ as well as the surface coverage. Note that in Figure 4, the flow rate in $^1$D is 0.037 mL/min, corresponding to $t_0$ of 59 min. Even with $t_G$ of 1180 min, the $t_G/t_0$ was 20 only. For the column used, the optimum flow is calculated to be ~0.167 mL/min (see Section 3.1). If we increase the column flow rate, for example to 0.15 mL/min, it will increase the column efficiency as it is closer to the optimum flow. In addition, it also decreases the $t_o$ which will increase $t_G/t_o$ to ~80 if keeping $t_G$ constant at 1180 min. Both the increase in column efficiency and $t_G/t_0$ are advantageous to achieve a large peak capacity (refer to Eq1 in the Introduction section), although it should be remarked the increase in peak capacity beyond values $t_G/t_0$ larger than 20 is merely incremental, as the steepest increase between $n_c$ and $t_G/t_o$ occurs for values of <10 [39,51]. The concern when using higher flow rates, however, is the decrease in loop fill time (=loop volume/$^1$D column flow rate). With a loop size of 40 µL and a flow rate of 0.15 mL/min, the loop fill time would be 0.27 min. In order to have a comprehensive 2-D run, the $^2$D cycle time must not be greater than the loop filling time (0.27 min in this case), which is too fast for the $^2$D column. To solve this dilemma, we applied the idea of a flow splitting after the $^1$D run [35]. In this approach, we could run the column at 0.15 mL/min, whilst splitting the column effluent after exiting the $^1$D detector using a Tee with a split ratio of 4:1 to direct only 0.030 mL/min flow to the loop in the ASM valve, as described in the Experiment section. This resulted in a loop filling time of 1.33 min.

The $^2$D cycle time in Figure 4 was 1.07 min with $t_G$ and $t_0$ of 0.83 and 0.082 min, respectively, with the column flow of 3 mL/min. To improve the $^2$D peak capacity, we could decrease $^2$D column flow to 1.7 mL/min to benefit from the higher column efficiency. The $t_0$, unfortunately, will increase to 0.145 min. To maintain $t_G/t_0$ of 10 and 2 times the $t_0$ hold in the end of the gradient for column flushing and 2 times the $t_0$ for column equilibration, the $^2$D cycle time turns into 2.02 min, which is greater than the loop fill time of 1.33 min if 40 µL sample loop in the ASM valve was used. To enable 1.7 mL/min flow in $^2$D, we changed the ASM valve loop to 70 µL, equating to 2.33 min of loop fill time, making it compatible with the $^2$D cycle time of 2.02 min.

As a consequence, we ran a next comprehensive 2-D LC by using flow rate of 0.15 mL/min and split ratio of 4:1 for $^1$D, 70 µL sample loop, 1.7 mL/min flow rate and cycle time of 2.02 min in $^2$D, and also slightly adjusting the mobile phase beginning and ending composition. The resulting 2D contour plot is shown in Figure 5. As expected, the $^1n_c$ and $^2n_c$ increased significantly, from 528 to 1263, and from 24.4 to 42.3, respectively, which corresponds to almost 4x gain in the apparent peak capacity ($^1n_c$ x $^2n_c$) from 13000 to 53000. The calculated effective peak capacity was significantly increased from 7600 to 11000 after correction for the surface coverage (0.82) and undersampling factor (4.0).

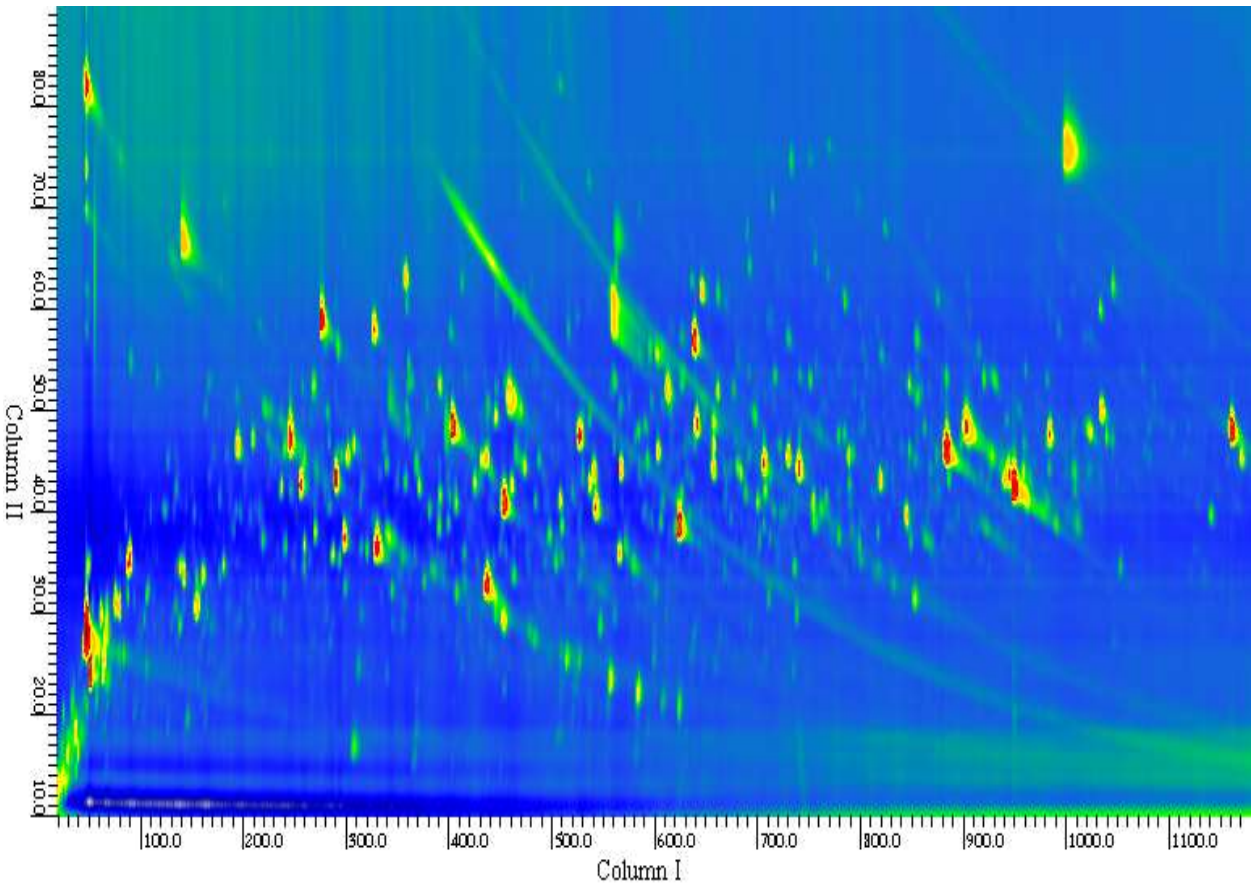


**Figure 5.** 2D LC contour plot of an aromatic amine sample using six F5 columns in $^{1}$D. Conditions: $^{1}$D, six coupled F5 column, 0.15 mL/min, with post-detector split of 4:1, 15-65% B over 1180 min, column temperature of 30 °C. Note that $t_0$ = 14.5 min. $^{2}$D, PAH column, 1.7 mL/min, 15-30% B in the beginning of 2D run (shifted to 70-100% over 1180 min in the ending of 2D run), the $^{2}$D gradient time of 1.59 min, cycle time of 2.02 min, column temperature of 50 °C.

To further demonstrate the advantage of high peak capacities produced when using six columns in $^{1}$D, a 2D run with only one F5 column in $^{1}$D and identical $^{2}$D condition, is shown in Figure 6. Adjusting the $t_G$ for the $^{1}$D to maintain the same $t_G/t_0$, the surface coverage is comparable, as expected. However, the resolving power was dramatically decreased resulting in many coelutions. This can be also readily assessed comparing the counted number of resolved peaks (350) for the one column case with the number of resolved peaks in six column case (940). From the perspective of industrial troubleshooting, this increase in number of resolved peaks more than warrants the longer analysis time.

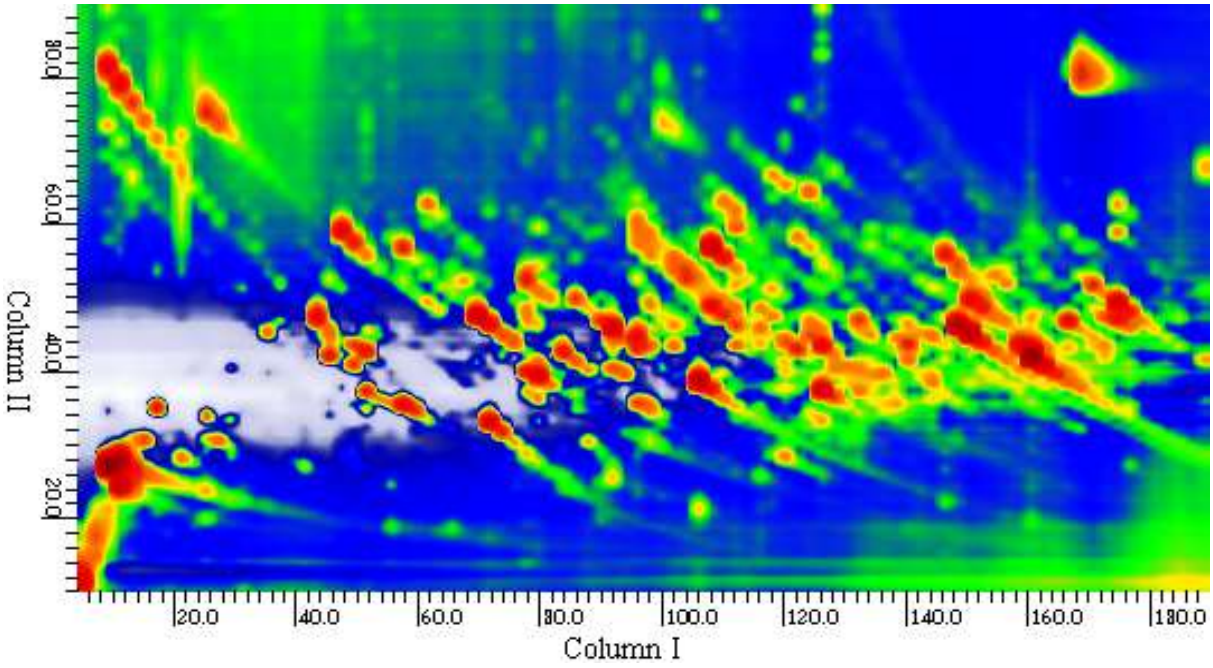


**Figure 6.** 2D LC contour plot of an aromatic amine sample using one F5 columns in $^{1}$D. Conditions: $^{1}$D, one coupled F5 column, 0.15 mL/min, with post-detector split of 4:1, 15-65% B over 196 min, column temperature of 30 °C. $^{2}$D conditions are the same as in Figure 5.

## 4. **Conclusions**

Peak capacity is the ultimate figure of merit for assessment of the resolving power of a chromatography system. Current state-of-the-art 1D liquid chromatography provides a maximum practical peak capacity of ~1000 with column void time of around 10 min using 1200 bar LC instrumentation. 2D LC, on the other hand, opens the possibility for an order improvement in peak capacity while separation time is still practical. We report on a study wherein we maximized the peak capacity by serially coupling up to six 15cm long 2.6 µm particle columns in the 1$^{st}$ dimension and 5 cm sub-2 µm column in the 2$^{nd}$ dimension using a commercially available 2D LC instrument capable of providing 1200 bar for each dimension. Several strategies were applied for the optimization of the 2D LC. The use of split flow in the $^{1}$D significantly improved its peak capacity while at the same time allowing relatively long cycle time be used in the $^{2}$D, which is also advantageous for improving the $^{2}$D peak capacity. Use of a more retentive polymeric C18 column in $^{2}$D allowed a large volume injection without detrimental volume overloading or solvent mismatch issue. Shift gradient was applied to dramatically improve the 2D surface coverage. Using an industrial aromatic amine oligomer sample under optimized conditions, we achieved overall peak capacity of 53000 and 11000, respectively, without and with correction for orthogonality and undersampling. Total analysis time with the 6-column system was around 20 hrs.

We observed 120 and 330 peaks in 1D separation using one or six columns, respectively. On the other hand, the 2D separation provided much more resolved peaks with 350 and 940 blobs for one column and six column case, respectively. Advantage of using six columns was clearly demonstrated for resolving complex industrial samples.

The potential of the sub-2 µm 5 cm long $^{2}$D column (peak capacity could be as high as 200) was not well realized due to fast flow for a comprehensive 2D LC run. Using shorter column in $^{2}$D could further improve the effective peak capacity by reducing the $^{2}$D cycle time to alleviate the undersampling, or increasing $t_G/t_0$.

**Acknowledgment**

We acknowledged the support of this study from the Nutrition & Health at DuPont, Analytical Sciences at The Dow Chemical Company and Department of Chemical Engineering at Vrije Universiteit Brussel.

**References:**


1. J.C. Giddings, Maximum number of components resolvable by gel filtration and other elution chromatographic methods, Anal. Chem. 39 (1967) 1027-1028.
2. J.W. Dolan, L.R. Snyder, N.M. Djordjevic, D.W. Hill, T.J. Waeghe, Reversed-phase liquid chromatographic separation of complex samples by optimizing temperature and gradient time. I. Peak capacity limitations, J. Chromatogr. A 857 (1999) 1-20.
3. J.H. Knox, M. Saleem, Kinetic conditions for optimum speed and resolution in column chromatography, J. Chromatogr. Sci. 7 (1969) 614-622.
4. H. Poppe, Some reflections on speed and efficiency of modern chromatographic methods, J. Chromatogr A 778 (1997) 3-21.
5. R.P.W. Scott, P. Kucera, Mode of operation and performance characteristics of microbore columns for use in liquid chromatography, J. Chromatogr. 169 (1979) 51-72.
6. H.G. Menet, P.C. Gareil, R.H. Rosset, Experimental achievement of one million theoretical plates with microbore liquid chromatographic columns, Anal. Chem. 56 (1984) 1770–1773.
7. K. Miyamoto, T. Hara, H. Kobayashi, H. Morisaka, D. Tokuda, K. Horie, K. Koduki, S. Makino, O. Nunez, C. Yang, T. Kawabe, T. Ikegami, H. Takubo, Y. Ishihama, N. Tanaka, High-efficiency liquid chromatographic separation utilizing long monolithic silica capillary columns, Anal. Chem. 80 (2008) 8741–8750.
8. J.E. MacNair, K.C. Lewis, J.W. Jorgenson, Ultrahigh-Pressure Reversed-Phase Liquid Chromatography in Packed Capillary Columns, Anal. Chem. 69 (1997) 983-989.
9. Y. Shen, R. Zhang, R.J. Moore, J. Kim, T.O. Metz, K.K. Hixson, R. Zhao, E.A. Livesay, H.R. Udseth, R.D. Smith, Automated 20 kpsi RPLC-MS and MS/MS with chromatographic peak capacities of 1000-1500 and capabilities in proteomics and metabolomics, Anal. Chem. 77 (2005) 3090-3100.
10. A. Vaast, J. De Vos, K. Broeckhoven, M. Verstraeten, S. Eeltink, G. Desmet, Maximizing the peak capacity using coupled columns packed with 2.6 µm core-shell particles operated at 1200 bar, J. Chromatogr. A 1256 (2012) 72-79.
11. J. De Vos, C. Stassen, A. Vaast, G. Desmet, S. Eeltink, High-resolution separations of tryptic digest mixtures using core-shell particulate columns operated at 1200 bar, J. Chromatogr. A 1264 (2012) 57-62.
12. J.M. Davis, J.C. Giddings, Statistical theory of component overlap in multicomponent chromatograms, Anal. Chem. 55 (1983) 418-424.
13. J.C. Giddings, Two-dimensional separations: concept and promise, Anal. Chem. 56 (1984) 1258A-1270A.
14. M.M. Bushey, J.W. Jorgenson, Automated instrumentation for comprehensive two-dimensional high-performance liquid chromatography of proteins, Anal. Chem. 62 (1990) 161-167.
15. I. Francois, D. Cabooter, K. Sandra, F. Lynne, G. Desmet, P. Sandra, Tryptic digest analysis by comprehensive reversed phase × two reversed phase liquid chromatography (RP-LC × 2RP-LC) at different pH's, J. Sep. Sci. 32 (2009) 1137-1144.
16. L. Mondello, P. Donato, F. Cacciola, C. Fanali, P. Dugo, RP-LC×RP-LC analysis of a tryptic digest using a combination of totally porous and partially porous stationary phases, J. Sep. Sci. 33 (2010) 1454-1461.
17. P.Q. Tranchida, P. Danato, F. Cacciola, M. Beccaria, P. Dugo, L. Mondello, Potential of comprehensive chromatography in food analysis, TrAC. 52 (2013) 186-205.

18. D. Li, C. Jakob, O. Schmitz, Practical considerations in comprehensive two-dimensional liquid chromatography systems (LCxLC) with reversed-phases in both dimensions, Anal. Chem. 407 (2014) 153-157.
19. G. Vanhoenacker, I. Vandenheede, F. David, P. Sandra, K. Sandra, Comprehensive two-dimensional liquid chromatography of therapeutic monoclonal antibody digests, Anal. Bioanal. Chem. 407 (2015) 355-366.
20. S. Kurono, Y. Kaneko, N. Matsuura, H. Oishi, S. Noguchi, S. Kim, Y. Tamaki, T. Aikawa, Y. Kotsuma, H. Inaji, S. Matsuura, Identification of potential breast cancer markers in nipple discharge by protein profile analysis using two-dimensional nano-liquid chromatography/nanoelectrospray ionization-mass spectrometry, Proteomics: Clinical Applications 10 (2016) 605-613.
21. M. Sarrut, F. Rouviere, S. Heinisch, Theoretical and experimental comparison of one dimensional versus on-line comprehensive two dimensional liquid chromatography for optimized sub-hour separations of complex peptide samples, J. Chromatogr. A 1498 (2017) 183-195.
22. V.R. Richard, D. Domanski, A.J. Percy, C.H. Borchers, An online 2D-reversed-phase - Reversed-phase chromatographic method for sensitive and robust plasma protein quantitation, J. Proteomics 168 (2017) 28-36.
23. U. Woiwode, R.J. Reischl, S. Buckenmaier, W. Lindner, M. Laemmerhofer, Imaging Peptide and Protein Chirality via Amino Acid Analysis by Chiral × Chiral Two-Dimensional Correlation Liquid Chromatography, Anal. Chem. 90 (2018) 7963-7971.
24. M. Kwiatkowski, D. Kroesser, M. Wurlitzer, P. Steffen, A. Barcaru, C. Krisp, P. Horvatovich, R. Bischoff, H. Schlueter, Application of Displacement Chromatography to Online Two-Dimensional Liquid Chromatography Coupled to Tandem Mass Spectrometry Improves Peptide Separation Efficiency and Detectability for the Analysis of Complex Proteomes, Anal. Chem. 90 (2018) 9951-9958.
25. M. Kivilompolo, V. Oburka, T. Hyotylainen, Comprehensive two-dimensional liquid chromatography in the analysis of antioxidant phenolic compounds in wines and juices, Anal. Bioanal. Chem. 391 (2008) 373-380.
26. P. Dugo, F. Cacciola, P. Danato, D. Airado-Rodriguez, M. Herrero, L. Mondello, Comprehensive two-dimensional liquid chromatography to quantify polyphenols in red wines, J. Chromatogr. A 1216 (2009) 7483-7487.
27. J.A. Raust, A. Brull, C. Morie, C. Farcet, H. Pasch, J. Chromatogr. A Two-dimensional chromatography of complex polymers, 1203 (2008) 207-216.
28. A.F.G. Gargano, M. Duffin, P. Navarro, P.J. Schoenmakers, Reducing Dilution and Analysis Time in Online Comprehensive Two-Dimensional Liquid Chromatography by Active Modulation, Anal. Chem. 88 (2016) 1785-1793.
29. B.W.J. Pirok, N. Abdulhussain, T. Aalbers, B. Wouters, R.A.H. Peters, P.J. Schoenmakers, Nanoparticle Analysis by Online Comprehensive Two-Dimensional Liquid Chromatography combining Hydrodynamic Chromatography and Size-Exclusion Chromatography with Intermediate Sample Transformation, Anal. Chem. 89 (2017) 9167-9174.
30. P. Yang, L. Bai, W. Wang, J. Rabasco, Analysis of hydrophobically modified ethylene oxide urethane rheology modifiers by comprehensive two dimensional liquid chromatography, J. Chromatogr. A 1560 (2018) 55-62.

31. M. Iguiniz, F. Rouviere, E. Corbel, N. Roques, S. Heinisch, Comprehensive two dimensional liquid chromatography as analytical strategy for pharmaceutical analysis J. Chromatogr. A 1536 (2018) 195-204.
32. M. Baert, S. Martens, G. Desmet, A. de Villiers, F. Du Prez, F. Lynen, Enhancing the Possibilities of Comprehensive Two-Dimensional Liquid Chromatography through Hyphenation of Purely Aqueous Temperature-Responsive and Reversed-Phase Liquid Chromatography, Anal. Chem. 2018, 90, 4961-4967.
33. S. Ji, S. Wang, H. Xu, Z. Su, D. Tang, X. Qiao, M. Ye, The application of on-line two-dimensional liquid chromatography (2DLC) in the chemical analysis of herbal medicines, J. Pharm. Biomed. Anal. 160 (2018) 301-313.
34. D.R. Stoll, X. Li, X. Wang, P.W. Carr, S.E.G. Porter, S.C. Rutan, Fast, comprehensive two-dimensional liquid chromatography, J. Chromatogr. A 1168 (2007) 3-43.
35. M.R. Filgueira, Y. Huang, K. Witt, C. Castells, P.W. Carr, Improving Peak Capacity in Fast Online Comprehensive Two-Dimensional Liquid Chromatography with Post-First-Dimension Flow Splitting, Anal. Chem. 83 (2011) 9531-9539.
36. A.I.A. Haidar, A. Soliven, R.C. Allen, M. Filgueira, P.W. Carr, Comparison of core-shell particles and sub-2 µm fully porous particles for use as ultrafast second dimension columns in two-dimensional liquid chromatography, J. Chromatogr. A 1386 (2015) 31-38.
37. K. Sandra, M. Steenbeke, I. Vandenheede, G. Vanhoenacker, P. Sandra, The versatility of heart-cutting and comprehensive two-dimensional liquid chromatography in monoclonal antibody clone selection, J. Chromatogr. A 1523 (2017) 283-292.
38. M.J. Davis, D.R. Stoll, P.W. Carr, Comparison of the Practical Resolving Power of One- and Two-Dimensional High-Performance Liquid Chromatography Analysis of Metabolomic Samples, Anal. Chem. 80 (2008) 268-278.
39. U.D. Neue, Peak capacity in unidimensional chromatography, J. Chromatogr. A, 1184 (2008) 107-130.
40. M. Gilar, P. Olivova, A.E. Daly, J.C. Gebler, Orthogonality of Separation in Two-Dimensional Liquid Chromatography, Anal. Chem. 77 (2005) 6426-6434.
41. J.M. Davis, D.R. Stoll, P.W. Carr, Dependence of Effective Peak Capacity in Comprehensive Two-Dimensional Separations on the Distribution of Peak Capacity between the Two Dimensions, Anal. Chem. 80 (2008) 8122-8134.
42. M.R. Schure, J.M. Davis, The statistical overlap theory of chromatography using power law (fractal) statistics, J. Chromatogr. A 1218 (2011) 9297-9306.
43. S.C. Rutan, J.M. Davis, P.W. Carr, Fractional coverage metrics based on ecological home range for calculation of the effective peak capacity in comprehensive two-dimensional separations, J. Chromatogr. A 1255 (2012), 1255, 267-276.
44. M. Camenzuli, P.J. Schoenmakers, A new measure of orthogonality for multi-dimensional chromatography, Anal. Chim. Acta. 838 (2014) 93-101.
45. B.W.J. Pirok, A.F.F. Gargano, P.J. Schoenmakers, Optimizing separations in online comprehensive two-dimensional liquid chromatography, J. Sep. Sci. 41 (2018) 68-98.
46. H. Gu, Y. Huang, P. Carr, Peak capacity optimization in comprehensive two dimensional liquid chromatography: A practical approach, J. Chromatogr. A 1218 (2011) 64-73.
47. G. Vivo-Truyols, S.J. van der Wal, P.J. Schoenmakers, Comprehensive study on the optimization of online two-dimensional liquid chromatographic systems considering losses in theoretical peak

capacity in first- and second-dimensions: A Pareto-optimality approach, Anal. Chem. 82 (2010) 8525-8536.
48. R.C. Allen, B.B. Barnes, I.A. Haidar Ahmad, M.R. Filgueira, P.W. Carr, Impact of reversed phase column pairs in comprehensive two-dimensional liquid chromatography, J. Chromatogr. A 1316 (2014) 169-177.
49. F. Bedania, W.T. Kok, H. Janssena, Optimal gradient operation in comprehensive liquid chromatography × liquid chromatography systems with limited orthogonality, Anal Chim. Acta 654 (2009) 77–84.
50. P. Jandera, T. Hajek, P. Cesla, Comparison of various second-dimension gradient types in comprehensive two-dimensional liquid chromatography, J. Sep. Sci. 33 (2010) 1382–1397.
51. L. Blumber, G. Desmet, Optimal mixing rate in linear solvent strength gradient liquid chromatography, Anal. Chem. 88 (2016) 2281−2288.